Nano Materials Science xxx (xxxx) xxx

Contents lists available at ScienceDirect

Nano Materials Science

journal homepage: www.keaipublishing.com/cn/journals/nano-materials-science/

SiO_2 decorated wood nanocomposite with enhanced mechanical performance, flame and water resistance

You-Yong Wang [a,b,1], Xiang-Qian Wang [b,1], Bei-Zhou Zhang [a], Shuai Zhai [a], Hao Li [a], Yuan-Qing Li [b,**], Wei-Bin Zhu [b,c], Shao-Yun Fu [b,*]

[a] School of Materials Science and Engineering, Hubei University of Automotive Technology, Shiyan 442002, China
[b] College of Aerospace Engineering, Chongqing University, Chongqing 400044, China
[c] Institute of Textiles and Clothing, The Hong Kong Polytechnic University, Hongkong 100872, China

ARTICLE INFO

Keywords:
Wood
SiO_2
Mechanical robustness
Fire resistance
Water resistance
Wear resistance

ABSTRACT

Development of lightweight and strong structural material using fast-growing poplar wood is promising for green and sustainable engineering. Herein, the overall performances of fast-growing natural poplar wood (NPW) are significantly enhanced via delignification, in situ growth of SiO_2 followed by densification. The SiO_2/compressed-delignified-wood (SiO_2/CDW) nanocomposite obtained exhibits outstanding mechanical properties including a bending strength of 395.6 MPa, a tensile strength of 253.4 MPa, and a toughness of 7.1 MJ/m^3, which is improved by 1548 %, 240 % and 590 %, respectively compared with NPW. In addition, the ignition time and burning time of SiO_2/CDW nanocomposite are prolonged by 700 % and 112 % compared to those of NPW. Moreover, the specific wear rate of SiO_2/CDW is 18×10^{-6} mm^3/Nm, which is 72.6 % lower than that of NPW. Moreover, the spring-back ratios of SiO_2/CDW in 95 % and in water are 45.2 % and 66.7 %, which are lower than those of CDW (64.6 % and 92.4 %). The SiO_2/CDW nanocomposite with enhanced mechanical, flame/water retardant and wear performances are promising to meet the needs of modern engineering as green and sustainable materials.

1. Introduction

In recent years, climate warming, depletion of oil resources and other crises severely threaten the green and sustainable development of human society. In this regard, the utilization of biomaterials, such as wood, is of great significance to the environmental protection and resource conservation [1–4]. Owing to the fast growth rate and high afforestation survival rate, fast-growing wood has great potential for wide applications, whereas its flammability and poor mechanical properties restrict their up-scale engineering applications [5,6]. Therefore, it is necessary to enhance the fire resistance and mechanical robustness of fast-growing wood, which is critical for improving the added value of fast-growing wood and decreasing the consumption of unsustainable resources. In addition, the friction and wear behaviors of woods have received much attention because they are likely to exhibit surface deformation behaviors under the coupling effects of poor working conditions, unsatisfactory lubrication conditions, and uneven impact forces in various engineering fields [7].

It is well known that impregnating polymer into the hierarchical porous structure of wood is effective to enhance its mechanical properties [8]. Such as, Frey et al. reported that the specific stiffness and strength of wood are dramatically enhanced by infiltrating epoxy into scaffold delignified wood followed by densification [9]. Yano et al. fabricated a wood/phenol formaldehyde composite by the combination of delignification, resin infiltration, and densification [10], which shows a higher Young's modulus and a two-fold increasement in flexural strength compared with natural wood. Meanwhile, impregnating polymer into wood is also effective to enhance its wear resistance. Such as, Kim et al. developed a wood/polyethylene glycol composite, which shows 20 % and 50 % reduction in specific wear rate and friction coefficient, respectively [11]. Liu et al. fills the pores of wood with lubricating oil to reduce its friction, resulting in a 50 % reduction in coefficient of friction and a stable friction process even after long-time friction [12]. Nevertheless, the utilization of petrol-based polymers loses the intrinsic environment friendliness of nature wood. Importantly, the introduction of polymers may further raise the fire safety concern of wood, because the

* Corresponding author.
** Corresponding author.
E-mail addresses: yqli@cqu.edu.cn (Y.-Q. Li), syfu@cqu.edu.cn (S.-Y. Fu).
[1] These authors contribute equally to this work.

https://doi.org/10.1016/j.nanoms.2024.09.005

flammable nature of most of polymers.

Compared with petrol-based polymers, many inorganic materials are non-combustible, environmentally friendly, and abundant in nature, which can be employed to improve the fire retardancy of wood. Gan et al. reported a fire-resistant wood based on the combination of densification and boron nitride nanocoating treatments, which exhibits a twofold increase in ignition delay time and a 25 % decrease in maximum heat release rate [13]. Inspired by matrix-mediated biomineralization, Merk et al. developed a strategy to enhancing the fire resistance of wood by deposition of $CaCO_3$ into the wood cell lumen [14,15]. Fu et al. impregnated the delignified balsa wood with colloidal montmorillonite clay to form a nanostructured wood hybrid, which also shows high flame-retardancy [16].

Silicon, which makes up about 25 % of the earth's crust, is the second most abundant element after oxygen. It is naturally found in form of mineral silicates, which mainly consist of polymeric SiO_2, which demonstrates a great potential for wood modification and protection [17]. Li et al. developed a wood/SiO_2 nanocomposite by in situ growth of nano-SiO_2 and densification of the wood substrate, which shows superhydrophobicity and good mechanical performance [18]. Dong et al. proposed a wood-based nanocomposite with higher specific strength and satisfactory durability by in situ generation of organic−inorganic hybrid polymer within wood via a sol−gel method [19]. Although surface coating and in situ growth of inorganic nanomaterials are effective in improving the fire resistance of wood, which are less effective in enhancing the mechanical properties of wood. It is clear that the wood modification strategies reported usually are effective for enhancing one specific property, while simultaneously enhancing the mechanical robustness, wear, water and fire resistance of wood remains a challenge.

In this work, as shown in Fig. 1a, a top-down strategy including delignification, in situ growth of SiO_2 followed by densification is proposed to fabricate wood-based nanocomposite. Firstly, nature poplar wood (NPW) is treated by NaOH & Na_2SO_3 solution to selectively remove lignin and hemicellulose, generating higher porosity in wood scaffold and exposing more hydroxyl groups [20]. Then SiO_2 nanoparticles are in situ synthesized in the delignified-wood scaffold by an sol-gel method. Finally, the delignified-wood with SiO_2 is densified with hot-pressing, and named as SiO_2/compressed-delignified-wood (CDW) nanocomposite. Compared with NPW, the SiO_2/CDW nanocomposite shows a 70 % reduction in thickness and displays significant improvement in mechanical properties, flame retardant and wear resistant performances simultaneously (Fig. 1b and c), which has a broad prospect in developing the green and sustainable society.

2. Experimental SECTION

2.1. Materials

Poplar wood is purchased from Luoyang timber market (Henan, China). The wood samples with a dimension of 90 × 10 × 20 mm^3 are dried at 103 ± 2 °C to minimize the water content. Sodium hydroxide (>97 %) and sodium sulfite (>98 %) are supplied by Aladdin Chemistry Co. Ltd. (Shanghai, China). Ethanol and tetraethyl orthosilicate (TEOS) are purchased from Chron Chemicals Co. Ltd. (Chengdu, China). γ-aminopropyltriethoxy silane (KH550, 98 %) is purchased from Yuanye Bio-Technology Co. Ltd. (Shanghai, China). Ammonium hydroxide solution ($NH_3{\cdot}H_2O$) is purchased from Chuandong Chemical Co. Ltd. (Chongqing, China).

2.2. Preparation of SiO_2/compressed-delignified-wood nanocomposite

Firstly, nature polar wood (NPW) is immersed in the boiling aqueous solution dissolved with 2.5 M NaOH and 0.4 M Na_2SO_3 for 12 h, followed by rinsing with boiling deionized water and freeze drying. Secondly, the

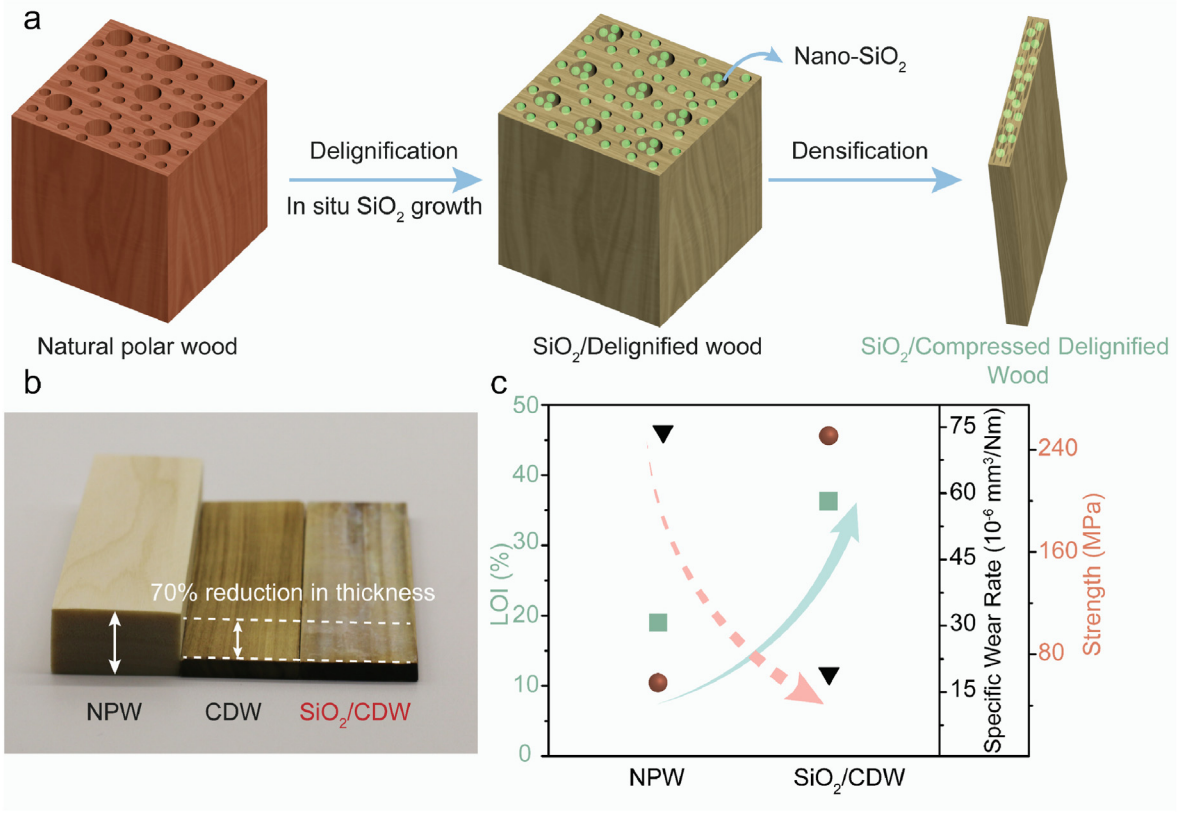

Fig. 1. (a) Schematic illustration of the fabrication process of SiO_2/CDW. (b) Dimension changes of CDW and SiO_2/CDW compared with NPW after treatment. (c) LOI, strength, and specific wear rate for NPW and SiO_2/CDW.

delignified and freeze-dried wood is placed in a chamber with constant temperature and humidity (30 °C, 80 ± 5 % relative humidity) for 12 h. Meanwhile, the SiO_2 precursor solution is obtained by mixing of TEOS, ethanol, and KH550 with a molar ratio of 1: 4: 0.1, and its pH is adjusted to 9 by the addition of $NH_3{\cdot}H_2O$ using a pipette drop by drop. Then the SiO_2 precursor solution is infiltrated into the delignified wood scaffold. Finally, the SiO_2/compressed-delignified-wood (SiO_2/CDW) nanocomposite is obtained by hot-pressing of the delignified wood scaffold containing SiO_2 at 100 °C and 15 MPa for 8 h. In addition, compressed-delignified-wood (CDW) is prepared for comparison by hot-pressing of the delignified wood at the same condition.

2.3. Characterization

The microstructure of NPW, CDW and SiO_2/CDW is imaged with a scanning electron microscope (SEM, Phenom, XL). The X-ray diffraction (XRD) pattern is obtained using a Rigaku RAPID II with a Cu Kα detector ($\lambda = 0.154\ 1$ nm) at 40 kV, 30 mA. The Fourier-transform infrared (FTIR) spectrum is recorded using a FTIR spectrometer (Thermo Nicolet, NEXUS 670). The mechanical properties of samples are tested using a universal testing machine (SANS, China). The tensile and three-point bending tests are performed at a loading rate of 5 and 2 mm min^{-1}, respectively. The sample dimensions for tensile and bending tests are 90 × 10 × 3 mm^3 and 50 × 10 × 3 mm^3, respectively. Toughness is calculated by the integration of tensile stress-strain curve [21]. Nanoindentation test is conducted with a Nano Indenter G200 system (Agilent Technologies). A Berkovich indenter is employed for the measurement based on a load-control method (400 mN). The dimension of sample for burning behavior test is 10 × 10 × 3 mm^3. Butane flame is used to ignite the wood sample. The thermogravimetric analysis (TGA) of NPW, CDW and SiO_2/CDW is performed by Netzsch-TG 209 F3 with a heating rate of 10 °C/min in N_2 atmosphere. Limited oxygen index (LOI) of wood samples is measured by a JF-3 oxygen index meter according to GB/T 2406.2-2009 with a dimension of 90 × 10 × 4 mm^3. The wear behavior of wood samples is evaluated by a wear test machine (Mazau, TRM 1000) in pin-on-disc configuration, according to the standard of ASTM G99-2005. The normal pressure, sliding velocity and sliding distance in wear test are set as 1 MPa, 1 m/s and 2 500 m, respectively. The sample is immersed into DI water or kept in a constant temperature and humidity box with 95 % relative humidity (RH) at 25 °C for 5 d to evaluate their water resistance. The size of the sample within 5 days is recorded. The spring-back ratio (SPR) is calculated according to the following equation:

$$SBR = (h_x\text{-}h_0)/(h_0/r)$$

where h_x is the thickness of the sample after treating for x h, h_0 is the untreated thickness after compression, and r is the compression ratio of

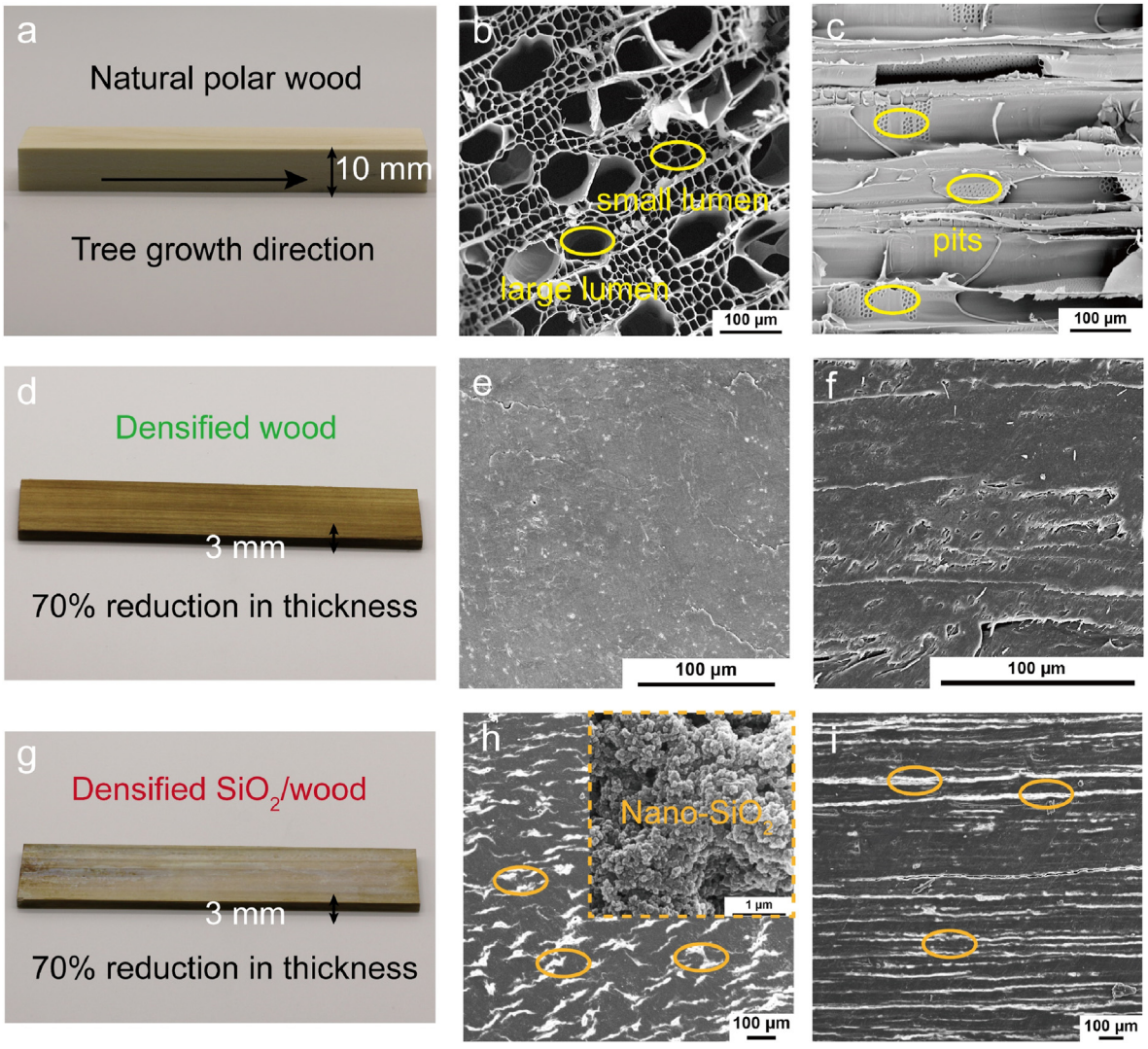

Fig. 2. Photographs: (a) NPW, (d) CDW and (g) SiO_2/CDW. SEM images: (b) NPW, (e) CDW and (h) SiO_2/CDW in radial direction; (c) NPW, (f) CDW and (i) SiO_2/CDW in growth direction. The insert of (h) is the morphology of nano-SiO_2.

CDW and SiO_2/CDW with respect to NPW.

3. Results and discussion

The macroscopic and microscopic structures of NPW, CDW, and SiO_2/CDW are presented in Fig. 2. The NPW sample has a slight brown color of nature wood, an initial thickness of about 10 mm (Fig. 2a), and a density of 0.37 g/cm^3. Meanwhile, a hierarchical porous structure is well observed in the radial direction of NPW (Fig. 2b). While many tubular channels with pits on the cell wall are seen in the tree growth direction (Fig. 2c), which would act as the mass transportation paths of SiO_2 precursor. CDW sample is prepared by delignification treatment and hot-pressing process. As shown in Fig. 2d, the CDW obtained shows a deep brown color and a 70 % reduction in thickness compared with NPW. At the same time, as demonstrated in Fig. 2e and f, the CDW nanocomposite in the tree growth direction and radial direction both exhibits a highly densified structure due to the hot-pressing treatment. As a result, the density of CDW is increased to 1.26 g/cm^3 (Fig. S1). Furthermore, the FT-IR spectra show that, after delignification treatment, the characteristic peaks of NPW at 1 235 cm^{-1} and 1 736 cm^{-1} corresponding to hemicellulose are disappeared, and the peak at 1 505 cm^{-1} corresponding to aromatic skeleton of lignin are weakened (Fig. S2), indicating that the hemicellulose and lignin in wood components are partially removed [22].

The thickness reduction of SiO_2/CDW nanocomposite is the same with that of CDW, while the color of SiO_2/CDW nanocomposite is relatively whiter than that of CDW, indicating the successful formation of SiO_2 (Fig. 2g). The SEM images show that SiO_2/CDW nanocomposite also exhibits a highly densified structure consistent with CDW. Meanwhile, homogeneously distributed bright areas are well observed on the fracture surface of SiO_2/CDW nanocomposite (Fig. 2h and i), and the magnified SEM image reveals that the bright areas are SiO_2 nanoparticles aggregated in the collapsed cell lumina, indicating the formation of a unique inorganic/organic hybrid structure. Organic components (cellulose) can act as the nucleation sites for SiO_2 growth. Compared with CDW, the density of SiO_2/CDW is slightly increased to 1.3 g/cm^3 due to the introduction of silica. The composition of SiO_2/CDW is further investigated. Results show that the weight content of SiO_2 is about 8.8 wt% and its volume fraction is about 5.2 vol%. SEM-EDX mapping indicates that Si element is uniformly distributed in wood scaffold and its weight percentage is about 2.5 wt% (Fig. S3).

As shown in the FTIR spectrum (Fig. S2), the characteristic peaks of SiO_2/CDW at 1050 cm^{-1} to 1100 cm^{-1} and 460 cm^{-1} are corresponding to the stretching and bending vibration of Si-O-C and Si-O-Si, respectively, which indicate the formation of covalent bonding between SiO_2 and cellulose [17,23]. In addition, as shown in Fig. S4, three peaks located at 16.5°, 22.5°, and 34.6° are observed from the XRD pattern of NPW, which are attributed to the cellulose's crystalline planes of (101), (002), and (040), respectively. In addition, XRD patterns of CDW and SiO_2/CDW are identical with that of NPW, indicating that the crystalline

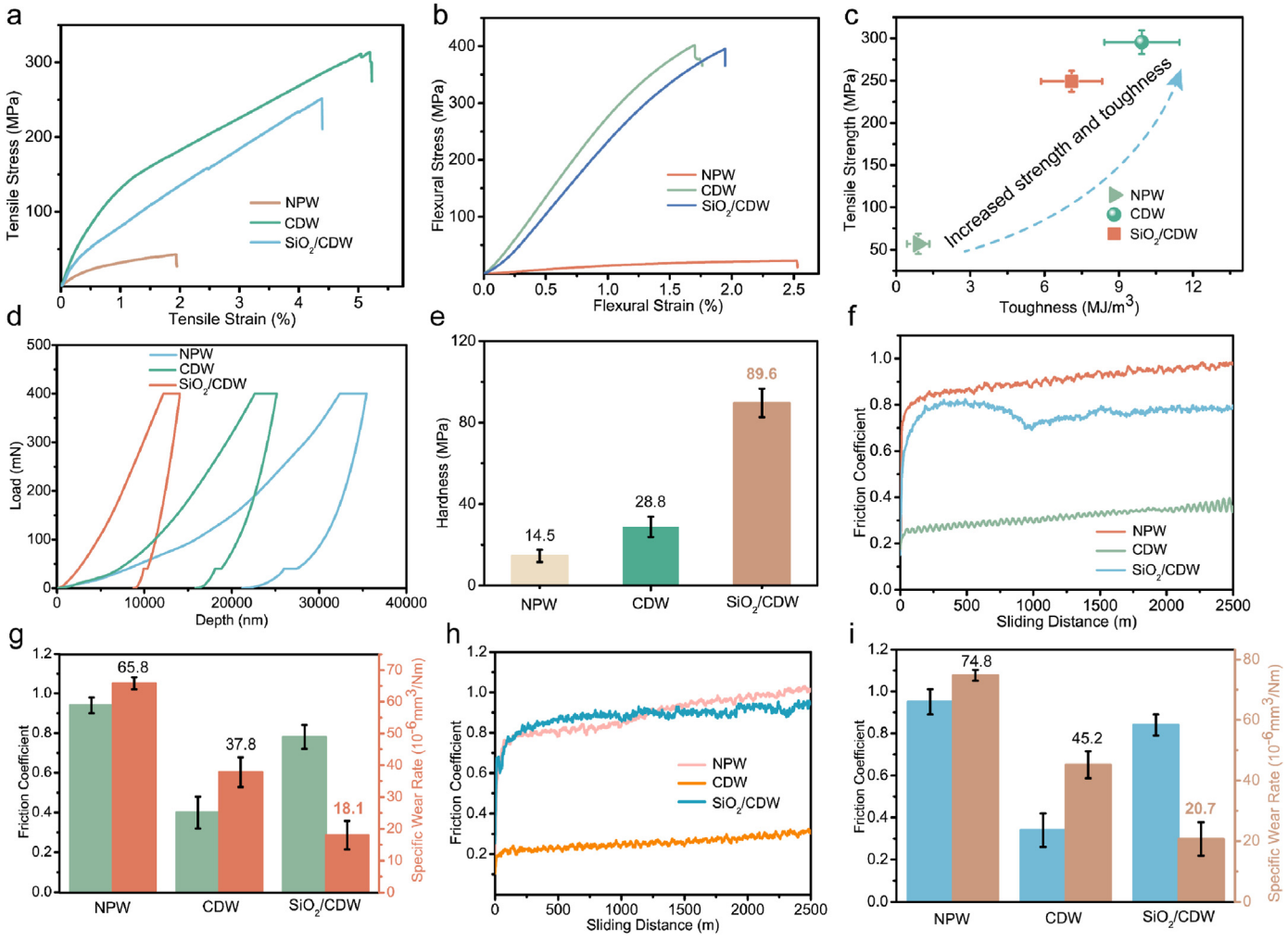

Fig. 3. Mechanical properties of NPW, CDW and SiO_2/CDW: (a) tensile stress-strain curve, (b) bending stress-strain curve, (c) tensile strength *vs* toughness, (d) loading-unloading curves of static nanoindentation tests, (e) hardness. Wear performances of NPW, CDW and SiO_2/CDW: (f, h) friction coefficient-sliding distance curves, and (g, i) friction coefficient and specific wear rate along the (f, g) growth direction and (h, i) radial direction of wood.

structure of wood cellulose does not change because of the retainment of cellulose I crystal structure in delignification without cellulose regeneration [24].

The effects of delignification, densification and in situ growth of SiO_2 on the mechanical properties of wood are investigated, and the tensile stress-strain curves of NPW, CDW and SiO_2/CDW are shown in Fig. 3a. The tensile strength of CDW reaches 313.6 MPa, which is increased by 619 % than that of NPW (43.6 MPa), and the tensile strength of SiO_2/CDW is 253.4 MPa, which is increased by 481 % than that of NPW. Meanwhile, the bending stress-strain curves of NPW, CDW and SiO_2/CDW are shown in Fig. 3b. The ultimate bending strength of CDW is 402.9 MPa, which is increased by 1579 % than that of NPW (24.0 MPa), and the bending strength of SiO_2/CDW is 395.6 MPa, which is increased by 1 548 % than that of NPW. The remarkable improvement in mechanical properties of CDW and SiO_2/CDW originates from delignification, densification and promoted hydrogen bonding. It should be pointed out that the mechanical properties of SiO_2/CDW are comparable to those of CDW, which indicates that the introduction of SiO_2 nanoparticles has negligible effect on the mechanical properties of wood. As shown in Fig. 3c, the toughness of CDW and SiO_2/CDW is about 9.9 MJ/m^3 and 7.1 MJ/m^3, respectively, which is increased by 1000 % and 689 %, respectively, compared with that of NPW (0.9 MJ/m^3). It is clear that the delignification and densification treatment is highly effective in improving the strength and toughness simultaneously, which is a long-term challenge in designing engineering materials [25]. Moreover, static nanoindentation tests are conducted to evaluate the hardness of woods, and the load-depth curves of NPW, CDW and SiO_2/CDW are shown in Fig. 3d. It can be seen that SiO_2/CDW displays the lowest depth of 8.8 μm, which is obviously lower than that of CDW (15.8 μm) and NPW (19.6 μm). As presented in Fig. 3e, the hardness of SiO_2/CDW is 89.6 MPa, which is 5.2 and 2.1 times higher than that of NPW and CDW, respectively.

The wear resistance of woods is critical for their application in floor and other friction related fields. Thus, the tribological behavior of NPW, CDW, and SiO_2/CDW are studied, and their friction coefficient and specific wear rate are calculated. Considering the anisotropy of wood, the friction and wear behaviors in the tree growth direction and the radial direction are investigated, respectively. The friction coefficient-sliding distance curves of NPW, CDW, SiO_2/CDW along the tree growth direction are shown in Fig. 3f. There is a period of running-in time before the state of steady friction due to the geometrical effect, deformation and material transfer [26]. NPW and CDW samples have pronounced running-in time in the range of 0 m to 100 m, and the friction coefficient value tends to stabilize subsequently. By contrast, SiO_2/CDW nanocomposite exhibits a longer running-in time up to 500 m. As displayed in Fig. 3g, in the steady state, the friction coefficient of NPW in the tree growth direction is 0.94. The high friction coefficient of NPW is attributed to its rough and porous structure. Compared with NPW, the friction coefficient of CDW is dropped to 0.4, because its highly densified structure results in a smooth friction surface. While the friction coefficient of SiO_2/CDW is further increased to 0.78 due to the increase of surface roughness caused by the introducing of SiO_2 nanoparticles. In addition, the CDW exhibits a specific wear rate of 37.8×10^{-6} mm^3/Nm, which is reduced by 42.5 % than that of NPW (65.79×10^{-6} mm^3/Nm) due to the lower friction coefficient and higher hardness of CDW. Importantly, the specific wear rate of SiO_2/CDW nanocomposite is as low as 18×10^{-6} mm^3/Nm, which is reduced by 72.6 % than that of NPW. The SiO_2 nanoparticles generated by in situ growth not only greatly improves the hardness, but also can heal the cracks produced by friction, which are responsible for the excellent wear resistance of SiO_2/CDW [27]. As shown in Fig. 3h, the friction coefficient-sliding distance curves of wood samples in the radial direction show the same tendency to that of in the tree growth direction. Similarly, the densification process reduces the friction coefficient of NPW (Fig. 3i), while in situ growth of SiO_2 nanoparticles increases the friction coefficient of CDW. Furthermore, the specific wear rate of SiO_2/CDW is 20.7×10^{-6} mm^3/Nm, which is far lower than those of NPW and CDW, demonstrating the effectiveness of SiO_2 nanoparticles in enhancing the wear resistance.

To evaluate the flame retardancy, the combustion behavior of NPW, CDW, and SiO_2/CDW under the butane flame are qualitatively studied. As shown in Fig. 4a, NPW is ignited within 2 s after being exposed to the flame, then burned violently with a strong flame, and extinguished at 33 s (Movie S1). After being exposed to the flame, CDW is ignited within 9 s, and the burning process is lasted to 47 s (Fig. 4b). Compared with NPW, the ignition time and burning time of CDW is prolonged to 9 s and 47 s, respectively, which attributes to the densified structure of CDW. It is known that char layer would be formed on the surface of burning wood [13]. Benefited with densified structure, the char layer of CDW is denser than that of NPW and the pyrolysis rate of CDW is lower than that of NPW concluded from the DTG curves (Fig. S5), which hinders the diffusion of oxygen and heat into the inner part of CDW, results in a delayed time to ignition and a prolonged burning time [28]. Noticeably, as shown in Fig. 4c and Movie S2, the SiO_2/CDW nanocomposite exhibits further delayed ignition time of 9 s and burning time of 70 s with self-extinguishing behavior. It is obvious that the inorganic SiO_2 nanoparticles formed by in-situ growth are incombustible, which can work as a flame retardant to improve the fire resistance of SiO_2/CDW nanocomposite.

To quantitatively evaluate the fire resistance of wood samples. The LOI of NPW, CDW, and SiO_2/CDW are tested. As displayed in Fig. 4d, the LOI values of NPW and CDW are 19.1 % and 27.9 %, respectively. Importantly, the LOI value of SiO_2/CDW is up to 36.7 %, which is increased by 130 % than that of CDW, and is the highest one among the wood composites reported in previous works [29–31]. In addition, the thermal stability of wood samples is evaluated by TGA. As shown in Fig. 4e, the initial pyrolysis temperature of NPW, CDW, and SiO_2/CDW is 272.3 °C, 250.2 °C, and 251.7 °C, respectively. At the same time, the temperature at maximum pyrolysis rate of SiO_2/CDW and CDW is 309.7 °C and 314.2 °C, respectively, which is also lower than that of NPW (354.8 °C). The decrease of pyrolysis temperatures may be attributed to the removal of lignin. DTG diagrams of NPW, CDW, and SiO_2/CDW indicate that the pyrolysis temperatures and rates of SiO_2/CDW and CDW are lower than that of NPW (Fig. S5). However, the residue char rate of CDW and SiO_2/CDW is 21.4 % and 28.9 %, respectively, which increases by 15.6 % and 56.2 %, respectively, compared with NPW (18.5 %), demonstrating that the densified structure and introducing of SiO_2 promote the formation char layer, and thus enhance the flame retardancy.

As structural materials, long term stability is critical in harsh environment like water attack. The dimensional stability of CDW and SiO_2/CDW is comparably studied under two conditions including 95 % RH and immersion in water. As shown in Fig. 5a, the thickness of CDW increased from 3.02 mm to 6.09 mm after being kept at 95 % relative humidity for 120 h, and the swelling ratio was 102 %; after being completely immersed in water for 120 h, the thickness increased by 3.15 mm, the swelling ratio was 206 %. While the thickness of SiO_2/CDW under the conditions of 95%RH and immersion in water is increased by 1.69 mm and 3.92 mm, respectively (Fig. 5b), the swelling ratio is 55.9 % and 129 %, respectively. In order to more accurately investigate the dimensional stability of CDW and SiO_2/CDW, we define the spring-back ratio to describe restore degree. Fig. 5c and d recorded the spring-back ratio of CDW and SiO_2/CDW in 95 % RH or immersion in water for various periods of time, respectively. It can be seen that CDW shows a spring-back ratio of 64.6 % at 120 h in 95 % RH. In contrast, the spring-back ratio of SiO_2/CDW is decreased to 45.6 % (Fig. 5c). When immersed in water, CDW quickly restored and stabilized. After 120 h, the spring-back ratio is up to 92.4 % (Fig. 5d). In contrast, the spring-back ratio of SiO_2/CDW is only 66.7 %, which is resulted from that inorganic SiO_2 framework can act as a barrier to hinder the diffusion of water molecules inside wood scaffold and reduce the water absorption rate. In summary, such excellent water resistance of SiO_2/CDW can remarkably improve the dimensional stability of wood and reduce water absorption under wet conditions.

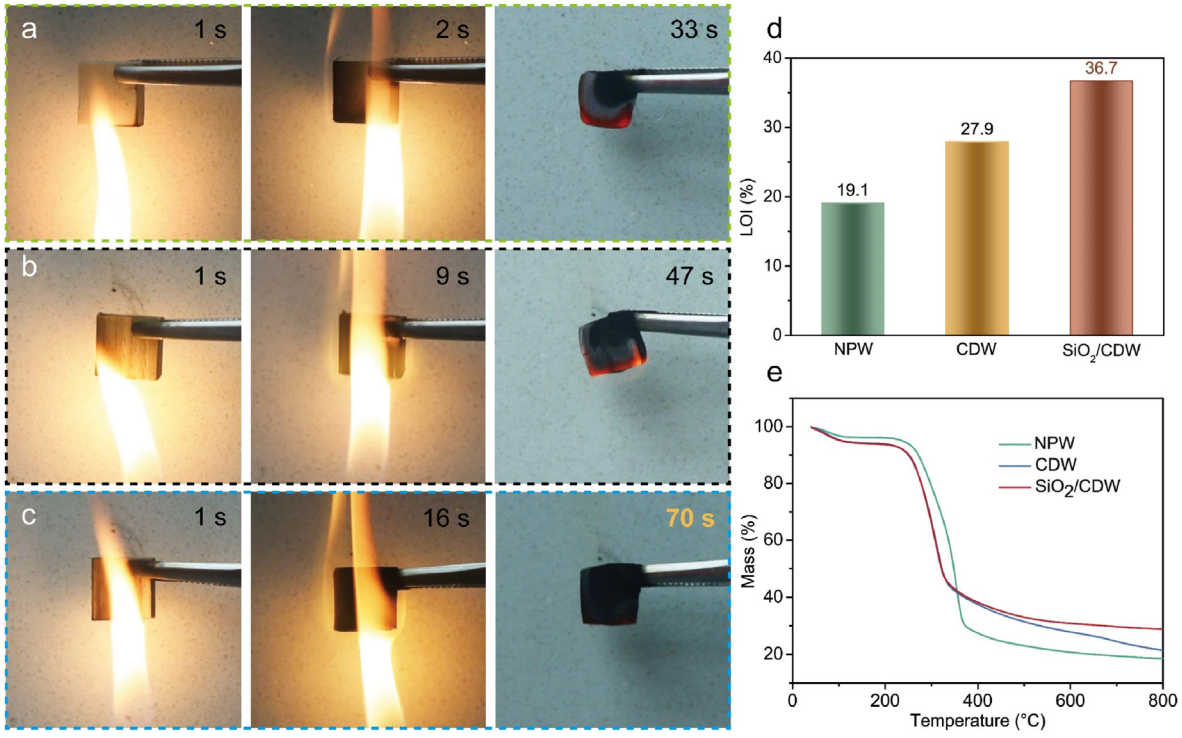

Fig. 4. Digital photographs of wood samples under burning: (a) NPW, (b) CDW and (c) SiO_2/CDW. (d) LOI and (e) TG curves of NPW, CDW, and SiO_2/CDW.

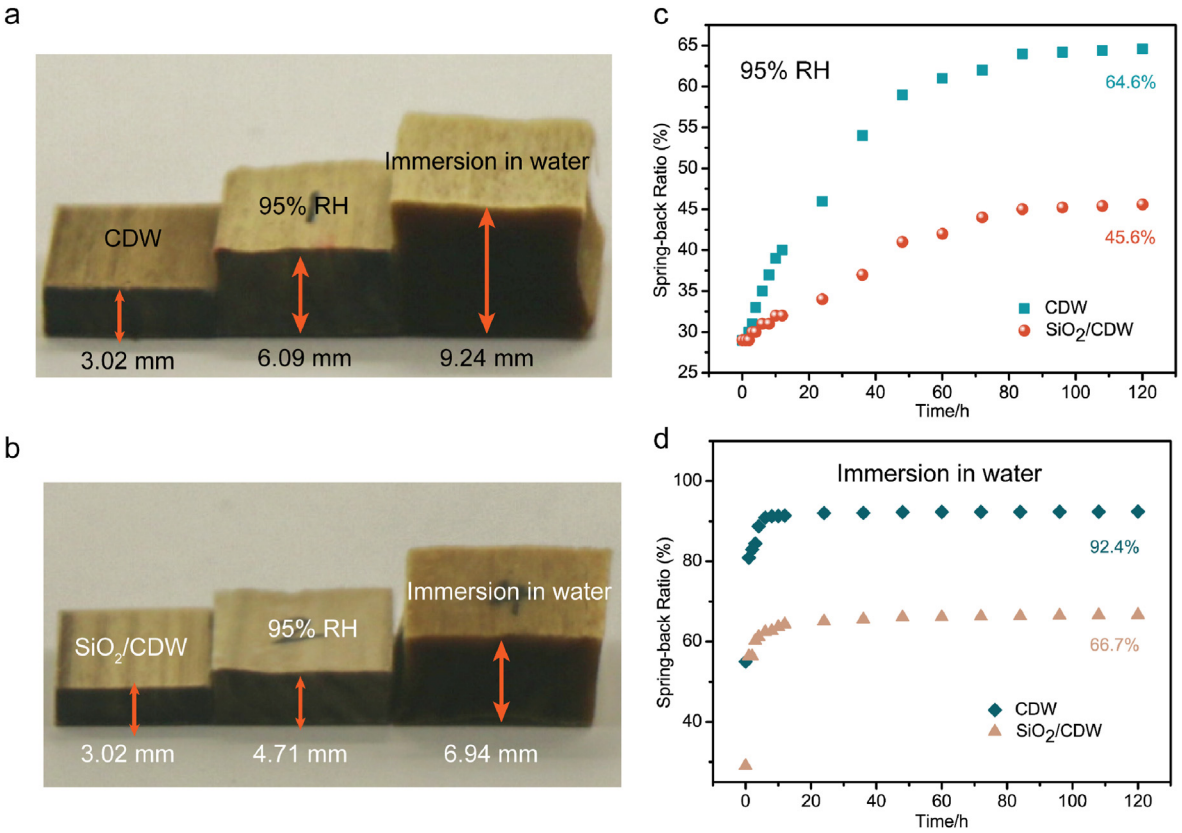

Fig. 5. Digital photographs of the thickness swelling in 95%RH and immersion in water for CDW (a) and SiO_2/CDW (b). Spring-back ratio of CDW and SiO_2/CDW in 95%RH (c) and immersion in water (d).

4. Conclusion

In summary, we develop a top-down strategy including delignification, in situ growth of SiO_2 followed by densification to process fast-growing NPW into a high performance SiO_2/CDW nanocomposite. The delignification treatment increases the porosity of natural wood with more hydroxyl groups exposed, which provides active sites for the growth of nano-SiO_2. After hot pressing, the SiO_2/CDW nanocomposite prepared exhibits a highly densified structure composed of SiO_2 nanoparticles and collapsed wood cell wall. As a result, the tensile and bending strengths of SiO_2/CDW are 253.4 MPa and 395.6 MPa, respectively, which are improved by 580 % and 1650 % than those of NPW, respectively. Moreover, the introducing of SiO_2 nanoparticles and highly densified structure endows excellent abrasion resistance and flame resistance to SiO_2/CDW. The specific wear rate of SiO_2/CDW is $18 \times 10^{-6} mm^3/Nm$, which is reduced by 72.6 % than that of NPW. When exposing to an open flame, the ignition time and burning time of SiO_2/CDW are prolonged by 700 % and 112 %, respectively compared with NPW. Moreover, the spring-back ratios of SiO_2/CDW in 95 % and in water are 45.2 % and 66.7 %, which are lower than those of CDW (64.6 % and 92.4 %). In consideration of the mechanically robustness, wear, fire and water resistance of SiO_2/CDW, the top-down strategy developed in this work is promising to process the fast-growing nature woods into green, sustainable, and high-performance engineering materials.

Notes

The authors declare no competing financial interest.

Authorship contributions

Youyong Wang: Conceptualization, Software, Validation, Writing-Original draft. Xiangqian Wang: Investigation, Data curation, Software, Validation. Beizhou Zhang: Data curation. Shuai Zhai: Data curation. Hao Li: Data curation. Yuanqing Li: Methodology, Writing-review & editing, Funding acquisition. Weibin Zhu: Investigation, Data curation. Shaoyun Fu: Supervision, Validation, Project administration, Funding acquisition.

Acknowledgments

The authors acknowledge the financial support from the National Natural Science Foundation of China (No. 52303082), Natural Science Foundation of Hubei Province (No. 2023AFB375), and Fundamental Research Funds for Central Universities of China (No. 2022CDJQY-004).

Appendix A. Supplementary data

Supplementary data to this article can be found online at https://doi.org/10.1016/j.nanoms.2024.09.005.

References

[1] Y.P. Chen, J.Z. Fu, B.K. Dang, Q.F. Sun, H.Q. Li, T.Y. Zhai, Artificial wooden nacre: a high specific strength engineering material, ACS Nano 14 (2) (2020) 2036–2043.
[2] F. Jiang, T. Li, Y. Li, Y. Zhang, A. Gong, J. Dai, et al., Wood-based nanotechnologies toward sustainability, Adv. Mater. 30 (1) (2018).
[3] Y.Y. Wang, X.Q. Wang, Y.Q. Li, P. Huang, B. Yang, N. Hu, et al., High-performance bamboo steel derived from natural bamboo, ACS Appl. Mater. Interfaces 13 (1) (2021) 1431–1440.
[4] W.-B. Zhu, Y.-Q. Li, J. Wang, Y.-Y. Wang, P. Huang, N. Hu, et al., High-performance fiber-film hybrid-structured wearable strain sensor from a highly robust and conductive carbonized bamboo aerogel, ACS Appl. Bio Mater. 3 (12) (2020) 8748–8756.
[5] L. Kong, H. Guan, X. Wang, In situ polymerization of furfuryl alcohol with ammonium dihydrogen phosphate in poplar wood for improved dimensional stability and flame retardancy, ACS Sustain. Chem. Eng. 6 (3) (2018) 3349–3357.
[6] J. Wang, S.J. Fishwild, M. Begel, J.Y. Zhu, Properties of densified poplar wood through partial delignification with alkali and acid pretreatment, J. Mater. Sci. 55 (29) (2020) 14664–14676.
[7] V. Rede, S. Essert, Z. Sokcevic, Effects of microstructural orientation on the abrasive wear resistance of subfossil elm wood in three orthogonal planes, Wear 380–381 (2017) 1–5.
[8] Y. Qin, Y. Dong, J. Li, Effect of modification with melamine–urea–formaldehyde resin on the properties of Eucalyptus and poplar, J. Wood Chem. Technol. 39 (5) (2019) 360–371.
[9] M. Frey, L. Schneider, K. Masania, T. Keplinger, I. Burgert, Delignified wood-polymer interpenetrating composites exceeding the rule of mixtures, ACS Appl. Mater. Interfaces 11 (38) (2019) 35305–35311.
[10] H. Yano, A. Hirose, P.J. Collins, Y. Yazaki, Effects of the removal of matrix substances as a pretreatment in the production of high strength resin impregnated wood based materials, J. Mater. Sci. Lett. 20 (12) (2001) 1125–1126.
[11] S.S. Kim, H.N. Yu, I.U. Hwang, D.G. Lee, Characteristics of wood-polymer composite for journal bearing materials, Compos. Struct. 86 (1–3) (2008) 279–284.
[12] S. Liu, C. Dong, C. Yuan, X. Bai, Friction reduction behavior of oil-infused natural wood, Friction 10 (11) (2022) 1824–1837.
[13] W. Gan, C. Chen, Z. Wang, Y. Pei, W. Ping, S. Xiao, et al., Fire-resistant structural material enabled by an anisotropic thermally conductive hexagonal boron nitride coating, Adv. Funct. Mater. 30 (10) (2020).
[14] V. Merk, M. Chanana, T. Keplinger, S. Gaan, I. Burgert, Hybrid wood materials with improved fire retardance by bio-inspired mineralisation on the nano- and submicron level, Green Chem. 17 (3) (2015) 1423–1428.
[15] V. Merk, M. Chanana, S. Gaan, I. Burgert, Mineralization of wood by calcium carbonate insertion for improved flame retardancy, Holzforschung 70 (9) (2016) 867–876.
[16] Q. Fu, L. Medina, Y. Li, F. Carosio, A. Hajian, L.A. Berglund, Nanostructured wood hybrids for fire-retardancy prepared by clay impregnation into the cell wall, ACS Appl. Mater. Interfaces 9 (41) (2017) 36154–36163.
[17] C. Mai, H. Militz, Modification of wood with silicon compounds. inorganic silicon compounds and sol-gel systems: a review, Wood Sci. Technol. 37 (5) (2004) 339–348.
[18] Y. Li, C. Chen, J. Song, C. Yang, Y. Kuang, A. Vellore, et al., Strong and superhydrophobic wood with aligned cellulose nanofibers as a waterproof structural material, Chin. J. Chem. 38 (8) (2020) 823–829.
[19] X. Dong, X. Zhuo, J. Wei, G. Zhang, Y. Li, Wood-based nanocomposite derived by in situ formation of organic–inorganic hybrid polymer within wood via a sol–gel method, ACS Appl. Mater. Interfaces 9 (10) (2017) 9070–9078.
[20] C. Jia, C. Chen, R. Mi, T. Li, J. Dai, Z. Yang, et al., Clear wood toward high-performance building materials, ACS Nano 13 (9) (2019) 9993–10001.
[21] M. Henriksson, L.A. Berglund, P. Isaksson, T. Lindstrom, T. Nishino, Cellulose nanopaper structures of high toughness, Biomacromolecules 9 (6) (2008) 1579–1585.
[22] Y. Li, Q. Fu, R. Rojas, M. Yan, M. Lawoko, L. Berglund, Lignin-retaining transparent wood, ChemSusChem 10 (17) (2017) 3445–3451.
[23] C. Mai, H. Militz, Modification of wood with silicon compounds. Treatment systems based on organic silicon compounds ? a review, Wood Sci. Technol. 37 (6) (2004) 453–461.
[24] E. Xu, Y. Zhang, L. Lin, Improvement of mechanical, hydrophobicity and thermal properties of Chinese fir wood by impregnation of nano silica sol, Polymers 12 (8) (2020).
[25] R.O. Ritchie, The conflicts between strength and toughness, Nat. Mater. 10 (11) (2011) 817–822.
[26] W. Luo, Q. Liu, Y. Li, S. Zhou, H. Zou, M. Liang, Enhanced mechanical and tribological properties in polyphenylene sulfide/polytetrafluoroethylene composites reinforced by short carbon fiber, Compos. B Eng. 91 (2016) 579–588.
[27] H. Li, S. Li, F. Li, Z. Li, H. Wang, Fabrication of SiO2 wrapped polystyrene microcapsules by Pickering polymerization for self-lubricating coatings, J. Colloid Interface Sci. 528 (2018) 92–99.
[28] W.T. Gan, C.J. Chen, Z.Y. Wang, J.W. Song, Y.D. Kuang, S.M. He, et al., Dense, self-formed char layer enables a fire-retardant wood structural material, Adv. Funct. Mater. 29 (14) (2019) 9.
[29] E.N. Kalali, L. Zhang, M.E. Shabestari, J. Croyal, D.-Y. Wang, Flame-retardant wood polymer composites (WPCs) as potential fire safe bio-based materials for building products: preparation, flammability and mechanical properties, Fire Saf. J. 107 (2019) 210–216.
[30] X. Li, D. Liang, K. Li, X. Ma, J. Cui, Z. Hu, Synergistic effect of a hypophosphorous acid-based ionic liquid and expandable graphite on the flame-retardant properties of wood–plastic composites, J. Therm. Anal. Calorim. (2020).
[31] Y. Yang, L. Haurie, J. Wen, S. Zhang, A. Ollivier, D.-Y. Wang, Effect of oxidized wood flour as functional filler on the mechanical, thermal and flame-retardant properties of polylactide biocomposites, Ind. Crop. Prod. 130 (2019) 301–309.